# Endoscopic endonasal bony landmarks of vertical petrous internal carotid: anatomic study

Sameh M. Amin, Hesham Fathy

Department of Otorhinolaryngology, Fayoum University, Faiyum, Egypt

Correspondence to Sameh M. Amin, MD, Department of Otorhinolaryngology Head and Neck Surgery, Fayoum University, Faiyum, 128 Gisr El Suis , Heliopolis, 11321, Egypt
Tel: +20 100 661 3574;
e-mails: abdelgalils @yahoo.com, drsamehmohamed71@gmail.com

**Received** 19 November 2017
**Accepted** 10 December 2017

**The Egyptian Journal of Otolaryngology**
2018, 34:9–14

**Background**
Endoscopic endonasal direct exposure or vascular control of basal internal carotid artery (ICA) is difficult among soft tissue of infratemporal fossa.
**Objective**
The aim of this work was to develop surgical instructional model for direct exposure of vertical petrous (Vp) ICA relatively dependent on bony fixed landmarks.
**Materials and methods**
Endoscopic endonasal drilling of 14 sides of dry skull models was presented. Different bony landmarks and measurements of Vp ICA canal were obtained.
**Results**
Endoscopic endonasal transpterygoid approach was performed. The medial pterygoid process and base were drilled to expose the vidian canal and foramen rotundum. The lateral pterygoid process was drilled following the slope of skull base to medial and lateral ends of foramen oval (FO). The spine of the sphenoid was drilled to obscure the tensor tympani canal and the bony Eustachian tube (ET). The bony end of ET was identified lateral to FO. The Vp ICA was exposed retrogradely by drilling the tubal process of tympanic bone (bone between FO and bony ET) downward, backward, and medially toward carotid foramen, forming an acute angle with horizontal petrous (Hp) ICA. The carotid foramen lies medial to styloid process. Three processes are identified sequentially from endonasal perspective; spine of sphenoid, tubal process of tympanic bone, and vaginal process of tympanic bone enclosing the styloid process laterally. The mean length of Vp ICA canal was 12.93±2.23 mm, mean width of FO was 5.04± 0.8 mm, and distance between FO and bony ET was 6.68±1.42 mm, representing surgical width of Vp ICA ~10 mm. The surgical corridor was ~10 mm wide and 15 mm long.
**Conclusion**
Endoscopic endonasal systematic orientation of bony fixed landmarks of Vp ICA exposure is described. The proposed endonasal bony pathway relatively bypasses the muscular compartment of infratemporal fossa. This model can help to obtain vascular control of basal ICA and retrograde identification of parapharyngeal ICA.

**Keywords:**
endonasal, endoscopic, skull base surgery, vertical petrous internal carotid artery

Egypt J Otolaryngol 34:9–14

1012-5574

## Introduction

In the era of expanded endonasal approaches (EEA), exposure of the basal internal carotid artery (ICA) remains a formidable task. Direct exposure of ICA is an essential part of nearly most sagittal and all coronal EEA [1]. The concept of using consistent bony landmarks in endoscopic and lateral skull base surgery is not new. These bony landmarks are useful to navigate the skull base, particularly in pathological conditions altering the anatomy. Preoperative radiological assessment of these bony landmarks is also feasible and less sophisticated in comparison with soft tissue landmarks [2]. Bony landmarks have been used thoroughly in literature to identify and/or expose different segments of ICA: opticocarotid recess, sellar bulge and carotid bulge for parasellar ICA, the clival recess for paraclival ICA, the vidian canal for lacerum ICA, foramen ovale (FO) for (Hp) ICA, and bony Eustachian tube (ET) for posterior genu [3–5]. The proximal part of basal ICA lies in the infratemporal fossa (ITF) before it enters the carotid canal to form the vertical petrous (Vp) ICA. Several studies have addressed the endonasal approach to ITF and parapharyngeal ICA [6]. However, limitations and difficulties of exposure and control of basal ICA in ITF include extensive adipose and pterygoid muscles dissection, pterygoid venous plexus, pterygoid osteotomies, posterior location in poststyloid compartment behind stylopharyngeus



 DOI: 10.4103/ejo.ejo_86_17

fascia, and close anterior location to internal jugular vein [7]. In comparison, Vp ICA lies inside a bony canal starting from carotid foramen at skull base till posterior genu at junction of Hp and Vp ICA, rendering exposure and vascular control theoretically more suitable. The authors therefore conducted this study in an attempt to develop a bony surgical instructional model of exposure of basal Vp ICA relatively avoiding extensive soft tissue infratemporal compartment.

## Materials and methods

Fourteen sides of dry adult dry skulls were drilled endonasally. The study did not include humans or cadaveric specimen. Regional ethical approval was obtained from the department of otorhinolaryngology Fayoum University, Egypt. The dry skull model was fixed in large holder (similar to temporal bone holder) in supine position with slight extension allowed during the dissection resembling endonasal endoscopic surgery. Nasal endoscope (Karl Storz and Co., Tuttlingen, Germany), 4 mm in diameter, 18 cm in length, exclusively with 0°, were used. Digital pictures were reproduced by coupling the endoscope to the video camera and using a computer capture system.

### Drilling technique

Endoscopic endonasal anterior and posterior ethmoidectomy was done using Kerrisons 1 and 2 mm. Penetration of basal lamella was done with microdrill whenever needed. In a dry skull base model, a wide middle meatalanatrostomy is readily available and was enlarged with uncinectomy and outfracture of inferior concha to obtain a wide direct 0° view of posterior wall of maxillary sinus. The superior concha and sphenoid ostium were identified, and a wide sphenoidotomy was done. Available sphenoid landmarks like opticocarotid recess, sellar bulge, and parasellar and paraclival ICA eminences were identified. The sphenopalatine foramen was detected in 0° endoscopic view behind ethmoidal crest of orbital process of perpendicular plate of palatine bone. The posterior wall of maxillary sinus was removed starting from its upper medial quadrant to expose Vidian canal, foramen rotundum, superior orbital fissure, and medial and lateral pterygoid processes. The parasellar region was exposed by thinning out the bone between later structures and wide sphenoidotomy. The pterygoid base was drilled between the vidian and foramen rotundum at pterygopalatine fossa and middle cranial fossa. The medial pterygoid process was drilled anteroinferior to vidian canal to gain more space. Slight head extension is needed at this level to obtain a comprehensive view. The lateral pterygoid process was drilled following its upper most part forming upward slope with skull base to reach the FO medial and lateral lips. The spine of sphenoid is lateral to FO, and its drilling is essential to better visualize the foramen spinosum (FS) at the skull base. Once FS is visualized properly in 0° endoscopic view two posterolateral bony canals become evident, the bony ET and tensor tympani bony canal above. The intervening bony plate between the FO and bony ET is the tubal process of tympanic bone. The Vp ICA canal was exposed retrograde by drilling the tubal process of tympanic bone downwards, backwards, and medially towards carotid foramen forming an acute angle with horizontal petrous (Hp) ICA. The carotid foramen lies medial to styloid process and cannot be visualized with 0° endoscopic view, except when tympanic bone is removed. Three processes are identified sequentially from endonasal perspective: spine of sphenoid, tubal process of tympanic bone, and vaginal process of tympanic bone enclosing the styloid process laterally. A coronal section of the dry skull was done just anterior to superior orbital fissure, and different measurements of Vp ICA canal and surrounding bony landmarks were taken using Vernier caliper. Figures 1–6 show dissection steps and orientation of bony landmarks in middle cranial fossa.

## Results

Our dissection using exclusively 0° endoscope emphasizes the drilling of lateral pterygoid plates and spine of sphenoid very close to skull base to visualize different bony landmarks especially bony ET. Tables 1 and 2 show dimensions of Vp ICA canal and distances of surrounding bony landmarks.

**Figure 1**

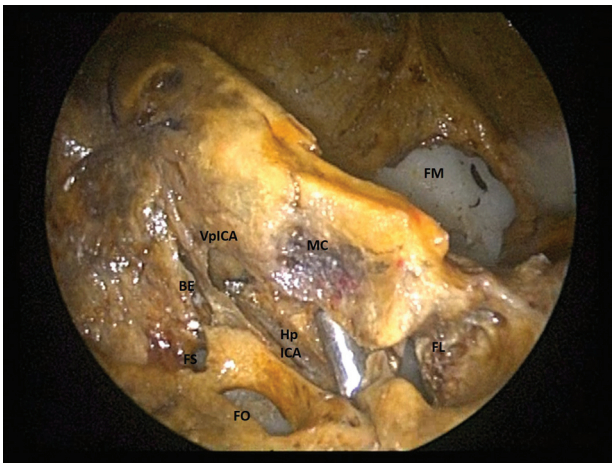


Superior view of middle cranial fossa showing relation of horizontal petrous ICA (HpICA) and vertical petrous ICA (VpICA) to foramen ovale (FO), foramen spinosum (FS) and bony Eustachian tube (BE). FM: Foramen Magnum, FL: foramen lacerum, MC: Meckels cave.

**Figure 2**

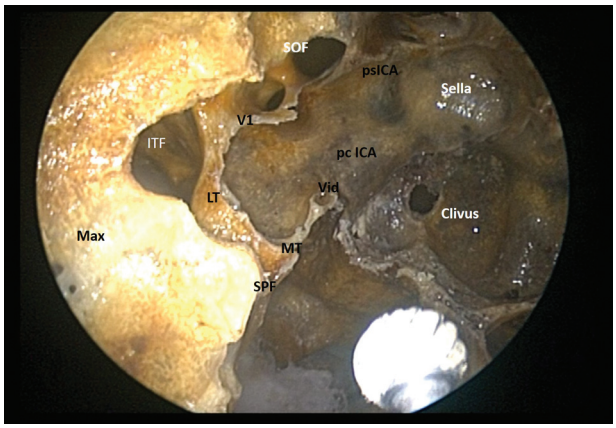


Endoscopic view of Rt sphenoid and parasellar region. After removal of posterior wall of maxilla, the SOF: superior orbital fissure, V1: Foramen rotundum, MT: medial pterygoid, LP: lateral pterygoid, Vid: Vidian canal, SPF: sphenpalatine foramen and ITF: infratemporal fossa can be identified. Sella, clivus, psICA: parasellar ICA, pcICA: paraclival ICA.

**Figure 3**

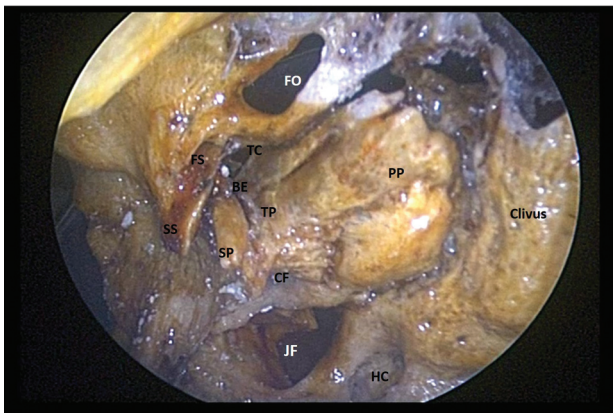


Endoscopic view after drilling of pterygoid base and medial and lateral pterygoids. The spine of sphenoid (SS) still obscuring foramen spinosum, bony Eustachian tube and tensor tympani canal (TC). The carotid foramen (CF) cannot be visualized due its anterior superior and lateral direction. The bone between FO: foramen oval and bony Eustachian tube (BE) is formed by tubal process of tympanic bone (TP). Laterally the tympanic bone gives a vaginal process to enclose the styloid process (SP). PP: Petrous pyramid, clivus, JF: Jugular foramen, FS: Foramen spinosum, HC: hypoglossal canal.

**Figure 4**

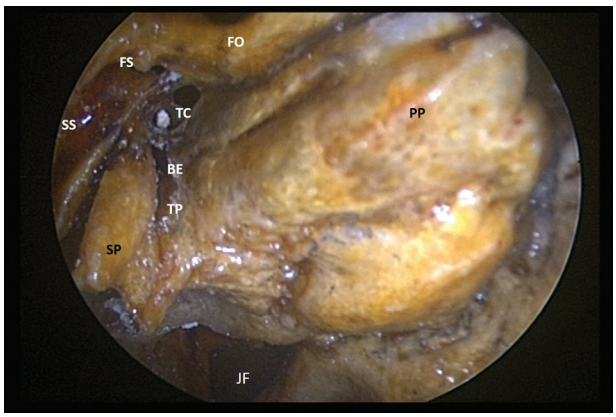


Endoscopic view after drilling the spine of sphenoid. The tensor tympani canal (TC) and bony Eustachian tube (BE) can be visualized with 0 degree endoscope.

**Figure 5**

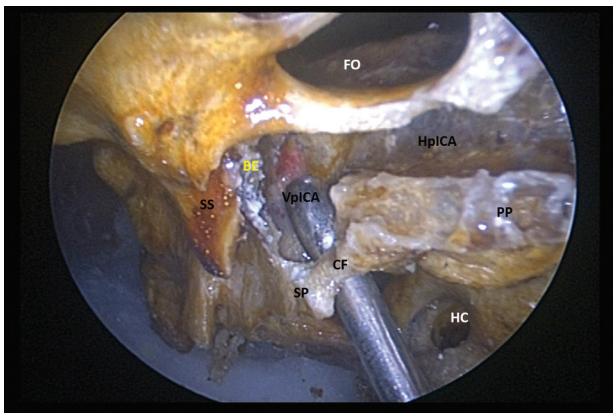


Endoscopic view after drilling the tubal process (TP) of tympanic bone to expose vertical petrous ICA (VpICA). The carotid foramen lies medial to styloid process (SP). Note the acute angle between VpICA and horizontal petrous ICA (HpICA). PP: petrous pyramid, BE: bony Eustachian tube, SS: spine of sphenoid, HC: Hypoglossal canal, FO; Foramen ovale.

**Figure 6**

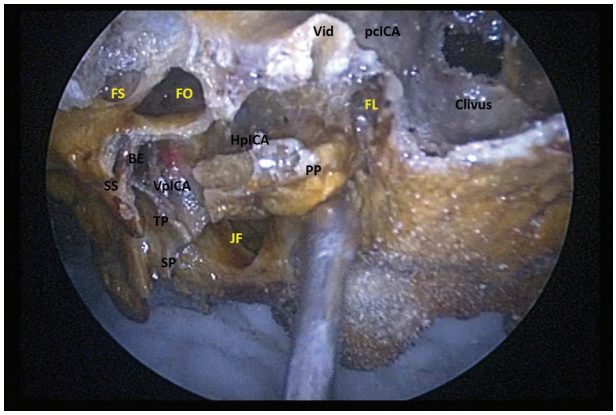


Endoscopic overview of petrous ICA. Clivus, PP: Petrous pyramid, VpICA: Vertical petrous ICA, HpICA: horizontal petrous ICA, JF: Jugular foramen, pcICA: paraclical ICA, Vid: Vidian Canal, FL: Foramen lacerum, FO: Foramen ovale, FS: foramen spinosum, TP: tubal process of tympanic bone, SP: Stylod process, SS: Spine of sphenoid, BE: Bony Eustachian tube.

## Discussion

In the era of EEA, the skull base surgeons become ambitious addressing pathologies in coronal plane including the ITF. Several anatomical studies focused initially on medial part of ITF for better management of sinonasal tumors extending to this region [8]. Thereafter, increased interest was directed to all compartments of ITF including poststyloid region either for surgical treatment of advanced extradural tumors or as a corridor for intradural pathology [9]. This led to concept of vascular control of parapharyngeal or basal ICA, e.g.

**Table 1 Measurements of the different bony landmarks of the vertical petrous internal carotid artery at the skull base in millimeters**

| | FR-FO[a] | Vidian canal length[b] | LPP-FO[c] | FO width[d] | FO-bony ET[e] | Bony ET-VICAC[f] | VICAC length[g] |
|---|---|---|---|---|---|---|---|
| Skull 1 | | | | | | | |
| Right | 18, 22 | 16.5 | 21 | 4.5 | 6 | 6.5 | 13.5 |
| Left | 20, 22 | 21.5 | 21 | 4.5 | 6.5 | 6 | 13.5 |
| Skull 2 | | | | | | | |
| Right | 16, 18 | 10.25 | 16 | 4.5 | 6.5 | 9 | 11 |
| Left | 17, 19 | 12 | 14 | 4 | 5 | 8 | 13 |
| Skull 3 | | | | | | | |
| Right | 8, 10 | 11 | 17 | 4 | 4 | 6 | 11 |
| Left | 10, 13 | 10.5 | 16 | 6 | 5 | 5.5 | 11 |
| Skull 4 | | | | | | | |
| Right | 18, 21 | 11 | 18 | 6 | 7 | 7 | 15 |
| Left | 12, 18 | 16 | 15 | 4 | 6 | 6 | 16 |
| Skull 5 | | | | | | | |
| Right | 14, 16 | 13 | 16 | 5 | 4 | 5 | 9 |
| Left | 16, 18 | 12 | 15 | 6 | 5 | 4 | 11 |
| Skull 6 | | | | | | | |
| Right | 15, 18 | 12 | 16 | 5.5 | 3.5 | 7 | 11 |
| Left | 18, 20 | 13 | 15 | 6 | 3 | 9 | 14 |
| Skull 7 | | | | | | | |
| Right | 17, 22 | 12 | 19 | 5 | 6.5 | 7.5 | 17 |
| Left | 14, 18 | 11.5 | 18 | 5.5 | 5 | 7 | 14 |

[a]Foramen rotandum to foramen ovale (medial end to medial end, lateral end to lateral end); [b]From vidian foramen at pterygopalatine fossa to vidian foramen at foramen lacerum; [c]Lateral pterygoid plate to foramen ovale; [d]Medial to lateral lip; [e]Foramen ovale to bony Eustachian tube; [f]Bony Eustachian tube to vertical internal carotid artery canal (surgical thickness of carotid canal); [g]Length of vertical internal carotid artery canal from bony Eustachian tube to inferior border of tympanic plate.

**Table 2 Descriptive statistics of the measurements of the different bony landmarks of the vertical petrous internal carotid artery at the skull base (all measurements in millimeters)**

| | Number of sides | Minimum | Maximum | Mean±SD |
|---|---|---|---|---|
| FR-FO MM[a] | 14 | 8 | 20 | 15.21±3.36 |
| FR-FO LL[b] | 14 | 10 | 22 | 18.21±3.45 |
| Vidian canal length | 14 | 10.25 | 21.5 | 13.01±3.06 |
| LPP-FO[c] | 14 | 14 | 21 | 16.93±2.2 |
| FO width[d] | 14 | 4 | 6 | 5.04±0.8 |
| FO-bony ET[e] | 14 | 3 | 7 | 5.21±1.25 |
| Bony ET-VICAC[f] | 14 | 4 | 9 | 6.68±1.42 |
| VICAC length[g] | 14 | 9 | 17 | 12.93±2.23 |

[a]Foramen rotandum to foramen ovale medial end to medial end; [b]Foramen rotandum to foramen ovale lateral end to lateral end; [c]Lateral pterygoid plate to foramen ovale; [d]Medial to lateral lip; [e]Foramen ovale to bony Eustachian tube; [f]Bony Eustachian tube to vertical internal carotid artery canal (surgical thickness of carotid canal); [g]Length of vertical internal carotid artery canal from bony Eustachian tube to inferior border of tympanic plate.

in cases of endoscopic nasopharyngectomy [10]. Studies have shown many limitation of endoscopic ITF approach particularly when exposure and or vascular control of parapharyngeal ICA is required. Limitations include extensive pterygoid adipose and muscle dissection, pterygoid venous plexus, osteotomies, deep position of ICA in poststyloid compartment behind stylopharyngeus fascia and close anterior relation to internal jugular vein [1]. Several authors proposed depending on indirect bony landmarks in ITF for location of ICA. These indirect bony landmarks (lateral pterygoid and mandibular condyle) predict proximity and not exact location of ICA and therefore are deemed impractical. In comparison, the Vp ICA lies inside a bony canal and therefore can serve the concept of safer vascular control in this region [7]. Accordingly, the authors propose in this study exposure and vascular control of Vp ICA, highlighting its osteology, dimensions, and surrounding bony landmarks.

The Vp ICA canal starts at the carotid foramen medial to styloid process ascending upward, forward, and laterally toward the medial end of bony ET forming almost an acute angle with horizontal ICA. Its length depends on the extent of lower border of tympanic

bone. In this study, the length of Vp ICA was 12.93 ±2.23 mm, which is similar to previous studies, in which the length varied from 10 to 13 mm [11–13]. Similarly, FO width (5.04±0.8 mm) was in agreement of other studies addressing different races [14]. The distance between FO and bony ET was 5.21±1.25. The width of FO added to distance between FO to bony ET was ~1 cm representing the width of the surgical field to expose the Vp ICA. The surgical corridor of Vp ICA endoscopic exposure was about 2 cm long and 1 cm wide, which seems surgically sufficient for drilling of bone, mobilization of ICA, and/or application of vascular clips. This study also provides the skull base surgeon with the Vp ICA inferior, medial, and posterior orientation making an acute angle with Hp ICA. This orientation is essential when performing drilling and exposure of this ICA segment.

Ozturk *et al*. [15] found at the region of FO and FS, the bone thickness between ET and ICA 2.7±1.2 and 1.72 ±0.7 mm, respectively. In this study, the distance between bony ET and ICA was larger 6.68 ±1.42 mm, as it was measured from the tubal process of tympanic bone (which represents the anterior boundary of bony ET isthmus). However, this represents the surgically oriented distance to be drilled of anterior and posterior walls of bony ET in order to expose the Vp ICA. The distance between FO and bony ET (which represents the nearest valid surgical bony landmark to ICA particularly the posterior genu) was 5.2 mm. Similar results were obtained in temporal bone sections where FO to ICA distance was 5.24±1.16 mm (range: 3.48–7.17 mm). Direct measurement of distance between FO and ICA is variable at different levels and therefore difficult to obtain exactly. This explains the different values obtained in other radiological and cadaveric studies ranging from 3.8 to 5.24 mm. On the other hand, our model was designed to expose the Vp ICA lateral to FO and not the Hp ICA behind FO. Interestingly, these authors found longer distance of FS in comparison with FO to ICA (5.2–5.34 mm). This probably suggests the safety of drilling the bone over Vp ICA as FS lies posterolateral to FO [15].

The average distance between FR and FO in available literature is around 2 cm. In this study, this distance, however, seemed smaller medially at 15.21±3.36 mm than laterally at 18.21±3.45 mm, forming eventually a triangle representing the pterygoid base and the lateral extension needed for the transpterygoid approach to reach the first landmark of Vp ICA [14]. Again the distance between the lateral pterygoid and FO (16.93 ±2.2 mm) was similar to results of Bryant *et al*. [16] and Ho *et al*. [7]. Interestingly Ho *et al*. [7] demonstrated that this distance is smaller close to skull base and larger at the level of nasal floor. This fact supports that staying close to skull base not only bypasses relatively the muscular compartment of the ITF but presents also a shorter pathway. The concept of shorter and nonmuscular pathway to basal ICA seems important when vascular control is intendeds [7,16].

The Vidian canal length showed wide variation from side to side and ranges from 10.25 to 21.5 mm. However, the mean Vidian canal length was 13.01± 3.06 mm. This wide variation was also documented in studies by Mato *et al*. [18] and Vescan *et al*. [17] in which Vidian canal varied from 14 to 18 mm. This variation in addition to the presence of fibrous attachment of ET, foramen lacerum and petroclival cartilage, and pharyngobasilar fascia makes exposure of ICA and or vascular control at this site unfavorable. Dissection at this region is better reserved for tumorous conditions or endoscopic anterior petrosectomy, occasionally needed for petroclival tumors [17,18].

The ET and ICA are very close at bony ET where they share same bony wall. Proximally and distally to bony ET, the exposure of ICA requires extensive soft tissue dissection. We therefore propose this direct bony model to identify the basal petrous ICA proximally or parapharyngeal ICA retrogradely. The model can be used also for vascular control of ICA according to surgical setting either proximally or distally. When performing EEA in sagittal planes, the parasellar and the paraclival segments are usually readily exposed. However, more proximal exposure of lacerum ICA segment is technically difficult owing to extensive attachments between ET, lacerum foramen, petroclival cartilage, and pharyngobasilar fascia. Addressing pathology in posterior coronal or infrapetrous skull base needs more proximal vascular control. The parapharyngeal ICA has been proposed by many authors; however, endoscopic endonasal ITF approach is lengthy, requiring extensive soft tissue dissection. In tumorous setting, the bony landmarks are far superior to soft tissue dissection in the context of safe navigation through ventral skull base [1]. A bony instructional model would probably facilitate direct and early identification of basal ICA before dealing with tumor in this compartment. Proximal and distal control of vital neurovascular structures before tumor resection, e.g. endoscopic nasopharyngectomy, allows radicality while minimizing complications.

One disadvantage of this study was the use of dry skull base model. Fresh cadavers provide more realistic

dissection conditions. However, in this study, the osteology of Vp ICA canal and its surrounding bony landmarks were of concern. Measurements between different bony landmarks were not affected by using dry skull model.

## Conclusion

Endoscopic endonasal systematic orientation of bony fixed landmarks of Vp ICA exposure is described. The proposed endonasal bony pathway relatively bypasses the muscular compartment of ITF. This model can help to obtain vascular control of basal ICA and retrograde identification of parapharyngeal ICA. The basic osteology data of Vp ICA from endonasal perspective are established. Further cadaveric feasibility studies are needed to assess the feasibility of the approach.

### Financial support and sponsorship

Nil.

### Conflicts of interest

There are no conflicts of interest.

## References

1 Fortes FS, Pinheiro-Neto CD, Carrau RL, Brito RV, Prevedello DM, Sennes LU. Endonasal endoscopic exposure of the internal carotid artery: an anatomical study. Laryngoscope 2012; 122:445–451.

2 Amin SM, Nasr AY, Saleh HA, Foad MM, Herzallah IR. Endoscopic orientation of the parasellar region in sphenoid sinus with ill-defined bony landmarks: an anatomic study. Skull Base 2010; 20:421–428.

3 Alfieri A, Jho HD. Endoscopic endonasal approaches to the cavernous sinus: surgical approaches. Neurosurgery 2001; 49:354–360. discussion 360-362.

4 Kassam AB, Vescan AD, Carrau RL, Prevedello DM, Gardner P, Mintz AH, *et al.* Expanded endonasal approach: vidian canal as a landmark to the petrous internal carotid artery. J Neurosurg 2008; 108:177–183.

5 Liu J, Pinheiro-Neto CD, Fernandez-Miranda JC, Snyderman CH, Gardner PA, Hirsch BE, *et al.* Eustachian tube and internal carotid artery in skull base surgery: an anatomical study. Laryngoscope 2014; 124: 2655–2664.

6 Dallan I, Lenzi R, Bignami M, Battaglia P, Sellari-Franceschini S, Muscatello L, *et al.* Endoscopic transnasal anatomy of the infratemporal fossa and upper parapharyngeal regions: correlations with traditional perspectives and surgical implications. Minim Invasive Neurosurg 2010; 53:261–269.

7 Ho B, Jang DW, van Rompaey J, Figueroa R, Brown JJ, Carrau RL, *et al.* Landmarks for endoscopic approach to the parapharyngeal internal carotid artery: a radiographic and cadaveric study. Laryngoscope 2014; 124:1995–2001.

8 Herzallah IR, Germani R, Casiano RR. Endoscopic transnasal study of the infratemporal fossa: a new orientation. Otolaryngol Head Neck Surg 2009; 140:861–865.

9 Falcon RT, Rivera-Serrano CM, Miranda JF, Prevedello DM, Snyderman CH, Kassam AB, *et al.* Endoscopic endonasal dissection of the infratemporal fossa: anatomic relationships and importance of eustachian tube in the endoscopic skull base surgery. Laryngoscope 2011; 121:31–41.

10 Al-Sheibani S, Zanation AM, Carrau RL, Prevedello DM, Prokopakis EP, McLaughlin N, *et al.* Endoscopic endonasaltranspterygoid naso-pharyngectomy. Laryngoscope 2011; 121:2081–2089.

11 Liu JK, Fukushima T, Sameshima T, Al-Mefty O, Couldwell WT. Increasing exposure of the petrous internal carotid artery for revascularization using the transzygomatic extended middle fossa approach: a cadaveric morphometric study. Neurosurgery 2006; 59 (Suppl 2):ONS309–ONS318. discussion ONS318-O NS319.

12 Keshelava G, Mikadze I, Abzianidze G, Kakabadze Z. Petrous carotid artery's in situ bypass: anatomic study. World J Surg 2008; 32:639–641.

13 Scerrati A, Ercan S, Wu P, Zhang J, Ammirati M. Intrapetrous internal carotid artery: evaluation of exposure, mobilization and surgical maneuvers feasibility from a retrosigmoid approach in a cadaveric model. World Neurosurg 2016; 91:443–450.

14 Youssef A, Carrau RL, Tantawy A, Ibrahim AA, Prevedello DM, Otto BA, *et al.* Clinical correlates of the anatomical relationships of the foramen ovale: a radioanatomical study. J Neurolsurg B Skull Base 2014; 75:427–434.

15 Ozturk K, Snyderman CH, Gardner PA, Fernandez-Miranda JC. The anatomical relationship between the eustachian tube and petrous internal carotid artery. Laryngoscope 2012; 122:2658–2662.

16 Bryant L, Goodmurphy CW, Han JK. Endoscopic and three-dimensional radiographic imaging of the pterygopalatine and infratemporal fossae: improving surgical landmarks. Ann Otol Rhinol Laryngol 2014; 123:111–116.

17 Vescan AD, Snyderman CH, Carrau RL, Mintz A, Gardner P, Branstetter B 4th, *et al.* Vidian canal: analysis and relationship to the internal carotid artery. Laryngoscope 2007; 117:1338–1342.

18 Mato D, Yokota H, Hirono S, Martino J, Saeki N. The vidian canal: radiological features in Japanese population and clinical implications. Neurol Med Chir (Tokyo) 2015; 55:71–76.